Highlights of Spanish Astrophysics XII, Proceedings of the XVI Scientific Meeting of the Spanish Astronomical Society held on July 15 - 19, 2024, in Granada, Spain. M. Manteiga, F. González Galindo, A. Labiano Ortega, M. Martínez González, N. Rea, M. Romero Gómez, A. Ulla Miguel, G. Yepes, C. Rodríguez López, A. Gómez García and C. Dafonte (eds.), 2025

The HαIr diagnostics of the Hydra I cluster

de la Casa, C. C.[1], Hess, K. M.[1,2,3], Verdes-Montenegro, L.[1] Kotulla, R.[4], Chen, H.[5,6], Jarrett, T. H.[7,6,8], Cluver, M. E.[8,9], De Daniloff, S. B.[10,11], Carignan, C.[6,12,13], Gallagher, J. S.[4], Gendron-Marsolais M.-L.[1,14], Kraan-Korteweg, R.C.[6], Ianjamasimanana, R. [1]

Affiliations are listed at the end of the paper

Abstract

We have undertaken a study of the star formation history of 218 galaxies in the Hydra I cluster with Hα-based star formation rates from measurements from the DECam camera of the Víctor M. Blanco 4-meter Telescope. We employed WISE infrared data as an independent measure of star formation and stellar mass for these 218 galaxies. We classified the galaxies as quenching, on the main sequence, or star-bursting based on trends observed for AMIGA isolated galaxies. The spatial and velocity distribution of the 28 starburst galaxies show a possible link between the large scale structure feeding the Hydra I cluster and their heightened star formation activity. Finally, the 17 starburst galaxies with neutral gas measurements from MeerKAT show disturbed HI disks that suggest an environmentally-triggered boost in star formation within the last 10^7 yr. Processes such as ram pressure stripping or tidal interactions may underlie this anomalous triggering of star formation.

1 Introduction

The question of how environment affects galaxy evolution and contributes to the halting of star formation still evades a conclusive answer. We need statistically relevant studies on how environment promotes quenching as a function of stellar mass in dense environments. The Hydra I cluster is an ideal laboratory for the study of star formation quenching modes in dense environments such as galaxy clusters. Hydra I has been observed to be relaxed [3] yet undergoing active processes of assembly and accretion of new galaxies from the filaments that connect it to other clusters in the Great Attractor superstructure [2]. This means that Hydra I hosts a combination of recently infalling and relaxed galaxies that can offer insight on star formation quenching pathways.

2 Star formation rates

We have selected 218 galaxies from the Hydra I cluster within the velocity range $v \in [2000, 6000]\, km/s$. That is, a velocity distribution of $3\sigma_{\rm HC}$ [6] ($\sigma_{\rm HC}$ = 620 km s^{-1} [14]) around $v_{\rm HC} = 3597$km/s (assuming $z_{\rm HC} = 0.012$ [6]). Our sample has both Hα and IR measurements from the DECam camera and the WISE survey, respectively. We refer to these 218 galaxies as the HαIr sample. 45/218 galaxies are upper limits in the optical due to lower S/N, continuum subtraction or the presence of very bright nearby sources. 99/218 are upper limits in the infrared due to the poorer sensitivity of the WISE W4 band or the presence of really bright sources.

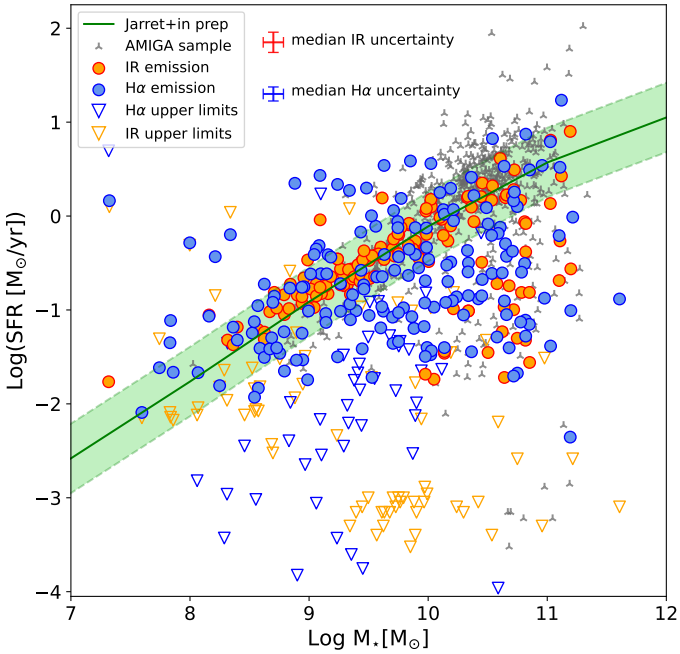

Figure 1: Star formation rate versus stellar mass of the HαIr sample, estimated from the IR (orange) and Hα (blue) emission respectively. Upper limits in optical and infrared are plotted as inverted triangles. The green region is the Main Sequence of star-forming galaxies that Jarrett+ in prep. fitted from a large sample from the 2MRS. The width of the Main Sequence was taken from AMIGA isolated galaxies from [1]'s fit of AMIGA isolated galaxies, which are shown in the background for reference (gray). Average uncertainties for detections in Hα and IR have been provided at the top of the diagram for clarity.

In Figure 1 we show the star formation rate (SFR) vs stellar mass ($M_\star$) computed for the HαIr sample. The blue points correspond to the $SFR_{\rm H\alpha}$ against the stellar mass derived from WISE, and the orange points correspond to the $SFR_{\rm IR}$ for the same galaxies, and therefore the same stellar masses. The former trace past star-forming activity at timescales of about $10^7 yr$, and the latter, up to $10^9 yr$. We can use this diagram to separate the HαIr sample in 3 different populations, according to $SFR_{\rm H\alpha}$:

1. Quenching Galaxies (QINGs): 75 detections + 41 upper limits ($\sim 53\%$ of HαIr galaxies) located below the Main Sequence ($SFR_{\mathrm{H}\alpha} < -\sigma$).
2. Main Sequence Galaxies (MSGs): 70 detections ($\sim 32\%$ of HαIr galaxies) on the Main Sequence ($-\sigma < SFR_{\mathrm{H}\alpha} < \sigma$). 1 upper limit is located in this region, so it is not possible to classify.
3. Starburst Galaxies (SBGs): 28/218 ($\sim 13\%$ of HαIr galaxies) above the Main Sequence ($SFR_{\mathrm{H}\alpha} > \sigma$). 3 upper limits are located in this region, so it is not possible to classify them.

A galaxy cluster in the state of relaxation in which Hydra I has traditionally been characterized [3] is expected to host a considerable population of quenching galaxies. In fact, previous studies focused on optical emission [11] found that almost 90% of Hydra I galaxies are quenched. However, the SBGs group seem to have undergone a dramatic increase in star formation rate. Not only is their $SFR_{\mathrm{H}\alpha}$ above the Main Sequence, but also $SFR_{\mathrm{H}\alpha} > SFR_{\mathrm{IR}}$. That is, instead of reducing their star formation rates, they must have sustained a burst in star formation in timescales shorter than $\sim 10^9$ yrs ago.

3 Cold gas morphology and spatial location of galaxies

Starburst in galaxies triggered by the effect of environment have already been observed in other clusters such as Coma [9], Fornax [13], or Virgo [10]. In all these cases, environmental processes easily identifiable by the asymmetries they produce in the gas disks of galaxies (ram pressure and tidal interactions are great examples) were behind the sudden increase in star formation activity.

Only 18/28 SBGs galaxies in our sample have HI detections from MeerKAT. However, all these 18 galaxies show this sort of asymmetries in their HI disks. In Fig. 2 (*left*) we show the Hα emission of the galaxy ESO 501-G053, an example of SBG from the HαIr sample, overlaid with HI contours. These contours show the kind of gas disk asymmetry that is typical in cases of ram pressure, even though the stellar content portrayed by the rgb image does not seem to be too altered. This finding is compatible with the results reported by [14], who employed WALLABY HI measurements in combination with optical Pan-STARRS bands to find that more than 70% of Hydra's galaxies with detectable levels of neutral gas within a virial radius are subjected to at least weak levels of ram pressure stripping, although the effects of such mild interactions were not certain.

Likewise, [12] examined the Hydra I cluster in combination with optical Pan-STARRS and infrared WISE data, and concluded that the environmental impact on the neutral gas reservoir can start as far as $1.5r_{200}$ from the cluster core. This implies that the impact of the cluster environment can start even before crossing its virial radius for the first time. Thus, the spatial and velocity location of galaxies with respect to the cluster core, and potential filaments feeding the cluster, is crucial to interpret the environmental processing and even the pre-processing that galaxies undergo in their orbits throughout the cluster and its surroundings.

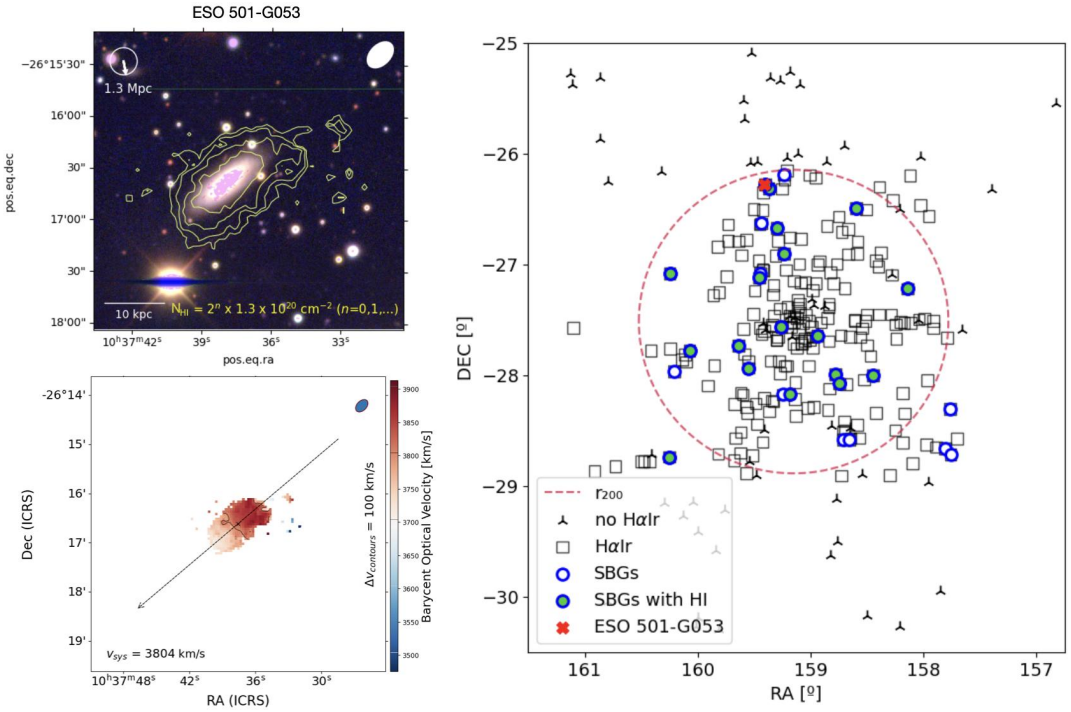

Figure 2: *Left:* ESO 501-G053, an example of SBG galaxy with asymmetrical HI disk. The upper plot shows an rgb composite (r,g,u bands from DECam) with an Hα map (magenta) and HI contours (yellow) overlaid. The compass at the top left corner indicates the direction to the cluster core, and the 2D projected distance to it is right below. The scale bar shows the 10kpc scale, and the yellow text contains the levels of the HI contours. The bottom diagram is an moment 1 velocity map of ESO 501-G053's HI content, elaborated with *SoFiA-Imaging-Pipeline (SIP). Right:* Distribution of galaxies in celestial coordinates. HαIr sample is represented with empty squares, and other Hydra I galaxies from 6dF galaxy survey are "triup" markers. SBGs have been represented as blue-edged-dots, and SBGs with an HI detection are colored green. The red cross indicates the location of ESO 501-G053.

In Fig. 2 (*right*) we have represented the spatial location of the galaxies within the HαIr sample, and highlighted the position of the SBGs in blue. 17/28 SBGs are located in the Southern half of the cluster, where HI detections are also slightly more abundant, and are generally blueshifted with respect to the cluster central velocity. This spatial asymmetry might be linked to an underlying structure feeding the cluster. New galaxies, far from entering symmetrically from all sides could be joining the cluster preferentially from the south. This view is further sustained by the fact that the Hydra cluster shares a filamentary connection with the southern Antlia cluster [8, 2], that serves as a bridge between these two clusters, which are separated $\sim 7.9°$ in the sky. This filament feeds Hydra from the South [5] (see

Figs. 10, 11, 12, 17, 18, 22 from [2]). This would explain how less active galaxies are usually found in the northern half, while those undergoing active or even bursting episodes of star formation are located to the south. Thus, the environmental transition from the filament to the cluster medium is a plausible origin for the SBGs increased star formation. Cases such as ESO 501-G053 might be galaxies that are passed their first pericenter in their orbit through the cluster, which would explain why its gas disk is more compressed in the direction opposite to the cluster core.

4 Conclusion

In view of the former results, we deduce that Hydra I has a dual nature. On one hand, it shows a population of mature and aged galaxies that follow the main sequence or that have already fallen from it. On the other hand, we find a population of what we believe are recently accreted galaxies undergoing a recent boost in their star formation caused by ram pressure or tidal interactions. These galaxies might be in their first orbits in the cluster after being newly accreted from the cosmic web or a filament (probably the Antlia-Hydra filament). These two complementary natures make Hydra an unique structure at large scale, both evolved and in active process of accretion of new material, and a promising laboratory for future multiwavelength studies.

Acknowledgments

The authors would like to acknowledge the tragic passing of co-author, Dr Thomas Jarrett. Authors C.C.C., K.M.H, L.V.M., M.L.G.M., R.I., acknowledge financial support from the grant CEX2021-001131-S funded by MICIU/AEI/ 10.13039/501100011033, and from the grant PID2021-123930OB-C21 funded by MICIU/AEI/10.13039/501100011033. Author C.C.C additionally aknowledges financial support from the grant TED2021-130231B-I00 funded by MICIU/AEI/ 10.13039/501100011033 and by the European Union NextGenerationEU/PRTR. K.M.H. and M.L.G.M. also acknowledges funding from the ERC under the European Union's Seventh Framework Programme (FP/2007-2013)/ERC Grant Agree- ment No 291531 ('HIStoryNU'). M.L.G.M. acknowledges financial support from the grant CEX2021-001131-S funded by MCIU/AEI/ 10.13039/501100011033, from the coordination of the participation in SKA- SPAIN, funded by the Ministry of Science, Innovation and Universities (MCIU), as well as NSERC via the Discovery grant program and the Canada Research Chair program. RCKK gratefully acknowledges partial funding support from the National Aeronautics and Space Administration under project 80NSSC18K1498, and from the National Science Foundation under grants No 1852136 and 2150222. RCKK greatly acknowledge support from the South African Research Chairs Initiative of the Department of Science and Technology and National Research Foundation. H.C. was supported by National Key R&D Program of China NO. 2023YFE0110500, and by the Leading Innovation and Entrepreneurship Team of Zhejiang Province of China (Grant No. 2023R01008). T.H.J. acknowledges support from the National Research Foundation (South Africa). M.E.C. acknowledges the support of an Australian Research Council Future Fellowship (Project No. FT170100273) funded by the Australian Government. S.B.D. acknowledges financial support from the grant AST22.4.4, funded by Consejería de Universidad, Investigación e Innovación and Gobierno de España and Unión Europea - NextGenerationEU, also funded by PID2020-113689GB-I00, financed by MCIN/AEI. J.S.G., is thankful for funding of this research provided by the University of Wisconsin-

Madison College of Letters and Science. Author C.C.C. acknowledges the Spanish Prototype of an SRC (SPSRC) service and support funded by the Ministerio de Ciencia, Innovación y Universidades (MICIU), by the Junta de Andalucía, by the European Regional Development Funds (ERDF) and by the European Union NextGenerationEU/PRTR. The SPSRC acknowledges financial support from the Agencia Estatal de Investigación (AEI) through the "Center of Excellence Severo Ochoa" award to the Instituto de Astrofísica de Andalucía (IAA-CSIC) (SEV-2017-0709) and from the grant CEX2021-001131-S funded by MICIU/AEI/ 10.13039/501100011033 [4]. The MeerKAT telescope is operated by the South African Radio Astronomy Observatory, which is a facility of the National Research Foundation, an agency of the Department of Science and Innovation. Part of the data published here have been reduced using the CARACal pipeline, partially supported by ERC Starting grant number 679627 "FORNAX", MAECI Grant Number ZA18GR02, DST-NRF Grant Number 113121 as part of the ISARP Joint Research Scheme, and BMBF project 05A17PC2 for D-MeerKAT. Information about CARACal can be obtained online under the URL: https://caracal.readthedocs.io [7]. We acknowledge the use of the ilifu cloud computing facility – www.ilifu.ac.za, a partnership between the University of Cape Town, the University of the Western Cape, Stellenbosch University, Sol Plaatje University and the Cape Peninsula University of Technology. The ilifu facility is supported by contributions from the Inter-University Institute for Data Intensive Astronomy (IDIA – a partnership between the University of Cape Town, the University of Pretoria and the University of the Western Cape), the Computational Biology division at UCT and the Data Intensive Research Initiative of South Africa (DIRISA). This work made use of the iDaVIE-v (immersive Data Visualisation Interactive Explorer for volumetric rendering) software (DOI – 10.5281/zenodo.4614116 – https://idavie.readthedocs.io. This work made use of the CARTA (Cube Analysis and Rendering Tool for Astronomy) software (DOI 10.5281/zenodo.3377984 – https://cartavis.github.io). This research has made use of the NASA/IPAC Extragalactic Database (NED), which is operated by the Jet Propulsion Laboratory, California Institute of Technology, under contract with the National Aeronautics and Space Administration.This research made use of *Photutils*, an Astropy package for detection and photometry of astronomical sources.

References

[1] Bok, J., Skelton, R. E., Cluver, M. E., et al. 2020, MNRAS, 499, 3193

[2] Courtois, H. M., Pomarède, D., Tully, R. B., Hoffman, Y., & Courtois, D. 2013, AJ, 146, 69

[3] Fitchett, M. & Merritt, D., 1988, AJ, 335, 18-34.

[4] Garrido, J., et al. 2020, JATIS: 011004-011004.

[5] Hess, K. M., Jarrett, T. H., Carignan, C., Passmoor, S. S., & Goedhart, S. 2015, MNRAS, 452, 1617

[6] Hess, K. M., Kotulla, R., Chen, H., et al. 2022, A&A, 668, p.A184.

[7] Józsa, G. I. G., White, S. V., Thorat, K., et al. 2020 ASCL: ascl-2006.

[8] Kraan-Korteweg, R.C., Woudt, P.A. & Henning, P.A. 1997 PASA, 14(1), 15–20

[9] Mahajan, S., Haines, C. P., & Raychaudhury, S. 2010, MNRAS, 404, 1745

[10] Mun, J. Y., Hwang, H. S., Lee, M. G., et al. 2021, arXiv preprint arXiv:2101.07472

[11] Lima-Dias, C., Monachesi, A., Torres-Flores, S., Cortesi, A., et al. 2021, MNRAS, 500(1), 1323-1339

[12] Reynolds, T. N., Catinella, B., Cortese, et al. 2021, MNRAS, 510(2), 1716-1732

[13] Serra, P., Maccagni, F., Kleiner, D., et al. 2023, A&A, 673,A146

[14] Wang, J., Staveley-Smith, L.,Westmeier, T., et al. 2021 TAJ: 915, 70.

[1] Instituto de Astrofísica de Andalucía (CSIC), Glorieta de la Astronomía s/n, 18008 Granada, Spain
[2] ASTRON, the Netherlands Institute for Radio Astronomy, Postbus 2, 7990 AA Dwingeloo, The Netherlands
[3] Department of Space, Earth and Environment, Chalmers University of Technology, Onsala Space Observatory, 43992 Onsala, Sweden
[4] Department of Astronomy, University of Wisconsin-Madison, 475 N Charter St, Madison, WI, 53706, USA
[5] Research Center for Astronomical Computing, Zhejiang Laboratory, Hangzhou 311100, China
[6] Department of Astronomy, University of Cape Town, Private Bag X3, 7701 Rondebosch, South Africa
[7] Institute for Astronomy, University of Hawaii at Hilo, 640 N Aohoku Pl 209, Hilo, HI 96720, USA
[8] Centre for Astrophysics and Supercomputing, Swinburne University of Technology, John Street, Hawthorn, 3122, Australia
[9] Department of Physics and Astronomy, University of the Western Cape, Robert Sobukwe Road, Bellville, 7535, South Africa [10] Dpto. de Física Teórica y del Cosmos, University of Granada, Facultad de Ciencias (Edificio Mecenas), 18071 Granada, Spain
[11] Institut de Radioastonomie Millimétrique (IRAM), Av. Divina Pastora 7, Núcleo Central 18012, Granada, Spain
[12] Département de physique, Université de Montréal, Complexe des sciences MIL, 1375 Avenue Thérèse-Lavoie-Roux, Montréal, Qc, Canada H2V 0B3
[13] Laboratoire de Physique et de Chimie de l'Environnement, Observatoire d'Astrophysique de l'Université Ouaga I Pr Joseph Ki-Zerbo (ODAUO), BP 7021, Ouaga 03, Burkina Faso.
[14] Département de physique, de génie physique et d'optique, Université Laval, Québec (QC), G1V 0A6, Canada